Utilization of Carbon Dioxide via Catalytic Hydrogenation Processes during Steam-Based Enhanced Oil Recovery

Authors:

Firdavs Aliev, Oybek Mirzaev, Temurali Kholmurodov, Olga Slavkina, Alexey Vakhin

Abstract:

The concentration of carbon dioxide in the atmosphere has been increasing since immediately after the boom of industrialization. Novel technologies are required for carbon dioxide (CO_2) capture, storage, and its chemical conversion into value-added products. In this study, we present a novel in situ CO_2 utilization method via a hydrogenation process in the presence of nickel tallates during steam-based enhanced oil recovery. The light n-alkanes are the preferred products of in situ catalytic hydrogenation of CO_2 due to their effective solubility, viscosity-reducing capacity, and hydrogen-donating capacity. A nickel tallate was evaluated for its carbon dioxide hydrogenation and oil-upgrading performance at 300 °C. The results showed that the content of saturated and aromatic fractions increased, while the content of heavier fragments decreased. Moreover, the relative content of normal C10?C20 alkanes doubled after the catalytic hydrogenation of CO_2. Despite the noncatalytic hydrogenation of CO_2, the viscosity was altered from 3309 mPa.s to 1775 mPa.s at a shear rate of 0.66 s?1. The addition of the catalyst further contributed to the reduction of the viscosity, down to 1167 mPa.s at the same shear rate. Thus, in situ catalytic hydrogenation of CO_2 not only significantly reduces the concentration of anthropogenic carbon dioxide gas in the atmosphere, but it also enhances the oil-recovery factor by improving the quality of the upgraded crude oil and its mobility.

Article

Utilization of Carbon Dioxide via Catalytic Hydrogenation Processes during Steam-Based Enhanced Oil Recovery

Firdavs Aliev [1],*, Oybek Mirzaev [1], Temurali Kholmurodov [1,2], Olga Slavkina [3] and Alexey Vakhin [1],*

1   Institute of Geology and Petroleum Technologies, Kazan Federal University, 420008 Kazan, Russia
2   Department of Chemistry, Samarkand State University, Samarkand 140104, Uzbekistan
3   RITEK LLC, 400048 Volgograd, Russia
*   Correspondence: aquathermolysis@gmail.com (F.A.); vahin-a_v@mail.ru (A.V.)

Abstract: The concentration of carbon dioxide in the atmosphere has been increasing since immediately after the boom of industrialization. Novel technologies are required for carbon dioxide (CO_2) capture, storage, and its chemical conversion into value-added products. In this study, we present a novel in situ CO_2 utilization method via a hydrogenation process in the presence of nickel tallates during steam-based enhanced oil recovery. The light n-alkanes are the preferred products of in situ catalytic hydrogenation of CO_2 due to their effective solubility, viscosity-reducing capacity, and hydrogen-donating capacity. A nickel tallate was evaluated for its carbon dioxide hydrogenation and oil-upgrading performance at 300 °C. The results showed that the content of saturated and aromatic fractions increased, while the content of heavier fragments decreased. Moreover, the relative content of normal C10–C20 alkanes doubled after the catalytic hydrogenation of CO_2. Despite the noncatalytic hydrogenation of CO_2, the viscosity was altered from 3309 mPa·s to 1775 mPa·s at a shear rate of 0.66 s^{-1}. The addition of the catalyst further contributed to the reduction of the viscosity, down to 1167 mPa·s at the same shear rate. Thus, in situ catalytic hydrogenation of CO_2 not only significantly reduces the concentration of anthropogenic carbon dioxide gas in the atmosphere, but it also enhances the oil-recovery factor by improving the quality of the upgraded crude oil and its mobility.

Keywords: heavy oil; carbon dioxide hydrogenation; CO_2 utilization; in situ conversion of CO_2; catalyst; nickel tallate; upgrading

1. Introduction

Carbon dioxide is considered to be the main anthropogenic greenhouse gas that contributes to global warming. According to the Paris Agreement (2015), the global roadmap was adjusted to reduce carbon dioxide emissions and to pursue efforts to limit global warming to 1.5 °C [1]. The petroleum industry is considered to be the largest source of CO_2 emissions. Many attempts have been made to capture and store carbon dioxide in depleted oil and gas reservoirs or salt domes [2–4]. Carbon dioxide has been applied widely to enhance oil recovery, particularly in cold production methods, for decades [5–7]. The main mechanisms that have led to the consideration of CO_2 as an efficient oil-displacing agent are as follows: Carbon dioxide favors crude-oil swelling, reduces oil viscosity, decreases interfacial tensions (IFTs), and exerts an acidic effect on reservoir rocks [8]. The physical consequences of CO_2 injection into oil reservoirs have been well-studied. However, the chemical interactions between CO_2 and hydrocarbons have been studied less due to thermodynamic stability of carbon dioxide. The conversion of CO_2 into value-added chemical products is often limited because of its high stability and the high strength of the C=O interaction. In the literature, it has been agreed upon that 192 kCal/mol of energy is required for the ionization of carbon dioxide [9]. However, it is well known that CO_2, under the appropriate conditions, can attract electrons to its empty orbital. Thus, substances that

bear high negative charges, such as anions, hydrogen-donating solvents, and hydrogen (H_2) gases, can react with CO_2 under high temperatures and pressures [10]. Hence, oil traps under steam-injection conditions are the cheapest natural reactors for utilizing carbon dioxide via hydrogenation. Moreover, hydrogenation products assist in further enhancing oil recovery via the formation of light n-alkanes and methane. The hydrogenation of carbon dioxide in the presence of catalyst particles has been studied widely, the products of which are valuable petrochemical raw materials, such as alcohols and various acids [11–13]. On the other hand, carbon monoxide (CO) can be obtained following (Equation (1)), the reverse water gas reaction (rWGS), as an intermediate product, whereas it is involved in Fischer–Tropsch hydrocarbon synthesis and Monsanto/Cativa acetic acid synthesis [14,15].

$$CO_2 + H_2 \leftrightarrow CO + H_2O \ (\Delta H \ 298K = 41.2 \ kJ/mol \ and \ \Delta G298K = 28.6 \ kJ/mol) \quad (1)$$
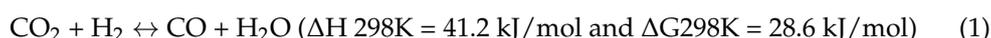
Although many papers have reported on the value-added products of carbon dioxide hydrogenation processes, the high conversion rate and selectivity of CO remains severe [16]. According to the literature, the most widely applied catalysts to promote rWSG and aquathermolysis reactions are based on Cu, Pd, Au, Pt, Ni, Re, Rh, Ru, Co, and Fe metals [17–19]. These catalysts have more or less been approbated under the atmospheric pressure and temperature range of 200–600 °C. Some authors have reported that Pd/Pt supported on ZnO, TiO_2, or SiO_2 shows lower activity (<20%) compared to Ni-, Rh- and Co-based catalysts supported on aluminum oxide (98–100% conversion) in terms of CO_2 hydrogenation, and they are more selective for methane formation [20–22]. Other authors expect a promising effect from applying Fe_2O_3-Cr_2O_3, which is widely used in industrial-scale WGS reactions, as well as in rWGS reactions [23–25]. The high performance of Fe-based catalysts in WGS reactions can be explained by the uncomplicated reduction in the oxidation states of iron (III) to iron (II). However, during the hydrogenation of carbon dioxide that requires a high temperature and pressure, the Fe_2O_3 phase can be reduced to metallic iron, which is less active in contrast to the iron oxides [24,26]. Hence, it is important to retain the oxide phase of iron-containing catalysts during the rWGS reactions. This can be achieved by the introduction of dopants, which contribute to the retention of the Fe_2O_3 phase. The use of catalysts based on nickel and cobalt in the rWGS reaction has been reported [27,28]. Iron-based catalysts, as a standard rule, withstand high temperatures. However, doping Ni/Co metals to the iron catalysts can be more active because of synergistic impacts between the doped and dopant metals. Dr. Changzhen Wang and his colleagues discuss the poor metal support of Ni-based catalysts in their paper [29]. They report that the active metal site does not withstand the high temperature, and hence, it loses its activity. The authors suggest improving the thermal stability of nickel catalysts by introducing phyllosilicate-derived core–shell nanomaterials.

To the best of our knowledge, there is no work in the literature that has studied the in-situ hydrogenation of CO_2 for enhancing oil recovery. The main objective of this article is to study the influences of in situ CO_2 utilization by catalytic hydrogenation process on steam-based enhanced oil recovery. For this purpose, we employed a sulfurous heavy oil sample with utter viscosity, a low degree of API (American Petroleum Institute) gravity, and a high content of resins and asphaltenes. The hydrogenation and upgrading performance of nickel tallate were evaluated during the steam treatment of heavy oil samples at 300 °C.

2. Materials and Methods

The heavy oil sample was classified as having a low degree of API gravity, being highly viscous, and being a high-sulfur crude oil. The injected carbon dioxide was 99% pure. The nickel-based catalyst precursor was obtained by the means of an exchange reaction between a sodium salt of tall oil and nonorganic salts of nickel. The technical details regarding the synthesis of the catalyst precursors are presented in our previous papers [30–32]. The obtained nickel tallate was further dissolved in a hydrogen-donating solvent with a mass ratio of 1:1.

The laboratory experiments imitating the in-situ utilization of CO_2 during steam stimulation were carried out in a high-pressure/high-temperature batch reactor (300 mL) with a stirrer manufactured by Parr Instruments, USA. First, 70 g of crude oil was loaded. Then, 30 g of water was added. The concentration of the catalyst precursor in the oil phase was 2 wt%. The reactor was purged for 15 min with CO_2 before the injection of 10 bar of CO_2 at room temperature. The whole closed system was checked for any leakage under the given pressure. The reactor was heated to 300 °C, and the time of reaction was 48 h. The HP/HT reactor was coupled with gas chromatography (GC), using the Crystal 5000 model, manufactured by Chromatec (Russia), which allows for the identification of the composition and quantity of evolved gases after the upgrading processes. The schematic illustration of the reactor model is presented in Figure 1.
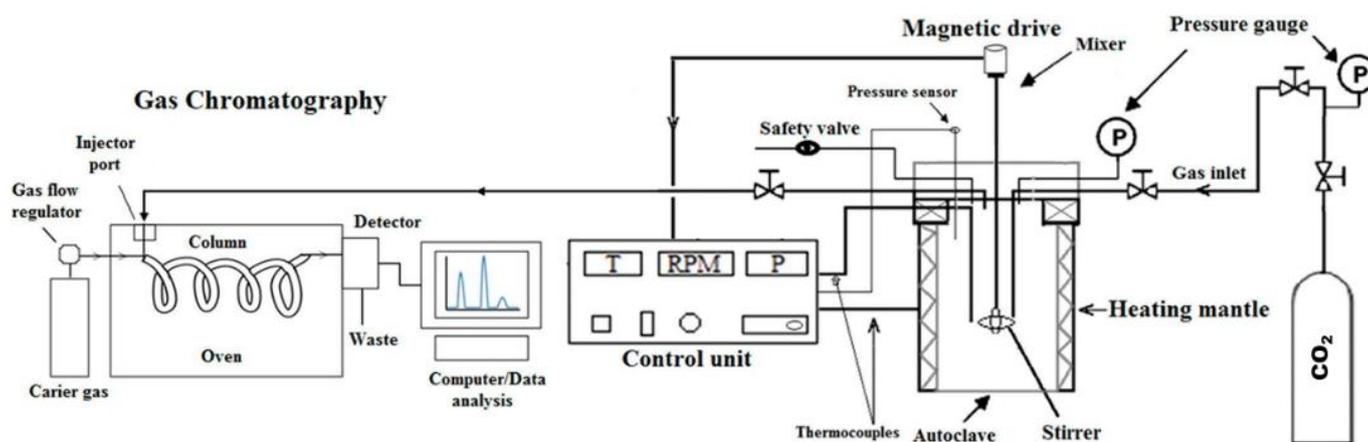

Figure 1. Schematic illustration of experimental setup.

The conversion products of CO_2 within the upgraded crude oil samples were isolated from the water by an Eppendorf 5804R centrifuge at 40 °C, with a rotation speed of 3000 rpm for 1 h. The upgrading products were further investigated via analytical methods.

The evolved gas was analyzed via gas chromatography using a Chromatec Crystal 5000.2 (Chromatec, Russia) with the Russian standard GOST 32507—2013, which is an analogue of ASTM D 5134-98 (2008), and further digital data processing. The gas fractionation was carried out by injecting a sample gas—helium—into a mobile phase and passing nanoparticles through it while supported inside a small-diameter metal tube with a length of 100 m. The temperature mode was set as follows: from 35 °C to 250 °C with a heating rate of 2 °C/min. The stream velocity was 15 mL/min.

The SARA analysis method was applied for the characterization of the group composition of the heavy oil by grouping saturates, aromatics, resins, and asphaltenes, following the regulations of Russian standard GOST 32269—2013—"Petroleum bitumen. Method of separation into four fractions". The isolation of the asphaltenes was carried out in a 40-fold quantity of an aliphatic solvent—heptane—with further extraction of the precipitated asphaltenes using a polar solvent in a Soxhlet apparatus. The elution of the saturates, aromatics, and resins was performed using heptane, toluene, and a mixture of toluene with carbinol (3:1), accordingly.

The light fractions of the crude oil samples, before and after the hydrogenation of the carbon dioxide, were examined using a GC-MS system, in which the GC "Chromatec-Crystal 5000" was coupled with a mass selective detector ISQ (USA). The data were processed using Xcalibur software. The temperature was increased from 100 °C to 150 °C at a rate of 3 °C/min, and from 150 °C to 300 °C at a rate of 12 °C/min, followed by its isotherm to the end of the analysis. The ionization energy was 70 eV, and the temperature of the ion source was 250 °C. The identification of the compounds was performed using the NIST Atomic Spectra Database and scientific publications.

The viscosity values of the initial crude oil sample and the crude oil samples after CO_2-assisted hydrothermal upgrading were calculated using a FUNGILAB Alpha L rotational viscometer (Valencia, Spain) equipped with a thermostatically controlled jacket. The required temperature in the thermal jacket was maintained using a HUBER MPC K6 cooling thermostat. All of the measurements were carried out by loading 6.7 mL of a heavy crude oil sample with a TL5 spindle. The shear rate for this spindle was determined by multiplying a 1.32 coefficient to the RPM value (according to the device's technical passport). The RPM was determined for a specific temperature and a spring torque of 50 to 90%. The relative error and the reproducibility of the FUNGILAB viscometer do not exceed $\pm 1.0\%$ and 0.2%, respectively.

The functional groups of the oil samples were studied using the FTIR analytical method. The IR spectrometer was designed by PERKIN ELMER, and the spectra of the oil samples were recorded with a single-reflection diamond in the range of 500–2000 cm^{-1}, with a resolution of 4 cm^{-1}. The spectral coefficients were estimated to quantitatively describe the aromaticity (C_1), oxidation (C_2), branching (C_3), aliphaticity (C_4), and sulfurization (C_5) of the oil samples, before and after CO_2-assisted hydrothermal upgrading. C_1 is the ratio of optical density values at the maxima of D1600/D720, indicating the stretching of C-C$_{aroma}$ bonds. The oxidation coefficient quantitatively represents the amount of carbonyl groups. The ratio of methyl and methylene groups to aromatic hydrocarbons stands for the aliphaticity, and the quantity of sulfoxide groups is evaluated as the sulfurization index.

3. Results and Discussion

3.1. The Composition of Evolved Gases

The results of the GC analysis revealed that most of the CO_2 in the absence of the catalyst is converted into methane (Table 1). The utilization degree of the CO_2 in the presence of the catalyst was increased from 5.75% to 10.74% due to the acceleration of the CO_2 hydrogenation reactions. Moreover, the catalyst promotes the hydrogen-donating capacity of both the steam and the solvent. In addition, the presence of the catalyst leads to the suppression of methane generation. On the contrary, it increases the formation of C_2–C_4 gases. The sum of these gases increased from 0.91% to 1.01%. The formation of methane can be explained by the Sabatier reaction, which is one of the proposed reaction paths for the interaction of hydrogen with carbon dioxide. On the other hand, the hydrogenation of CO_2 into the hydrocarbon gases in the presence of the catalyst can be considered as the modification of the Fischer–Tropsch process, whereby CO is replaced by CO_2. The evolved CO gas in the presence of the catalyst indicates that the rWGS mechanism is also involved during the in-situ utilization of CO_2 via hydrogenation processes. These reaction paths are summarized in Figure 2. The significant release of nitrogen gases (almost seven times greater, in contrast to the noncatalytic hydrothermal treatment) after catalytic hydrothermal treatment shows the efficiency of the catalyst on the denitrogenation of the heavy crude oil sample.

Table 1. The gas components which evolved after the noncatalytic and catalytic hydrothermal processes.

Model System *	Temp., C	Gas Yield (vol.%)										
		C_1	C_2	C_3	C_4	H_2	CO_2	H_2S	CO	O_2	N_2	Unidentified HC Gases
2	300	1.44	0.42	0.33	0.16	0.13	94.25	1.29	-	0.01	0.67	1.3
3	300	0.46	0.46	0.42	0.13	0.18	89.26	0.32	0.25	0.87	4.68	2.97

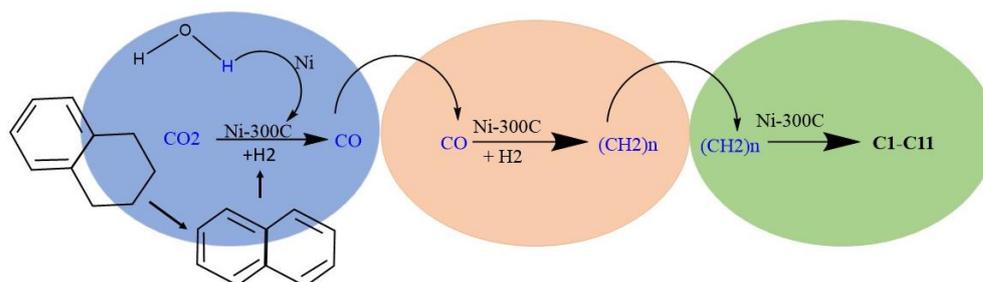* Model system: 2—Oil + Steam + CO_2; 3—Oil + Steam + Ni + CO_2.

Figure 2. The proposed in situ hydrogenation of CO_2 into light n-alkanes.

3.2. The Group Composition of Upgraded Crude Oil

The hydrogenation of CO_2 results in the group chemical changes in the composition of the crude oil sample (Figure 3). The noncatalytic hydrothermal treatment of heavy oil led to the polymerization of the resins, which could have been followed by an alteration in the content of the resins and the elevation of the fraction of the asphaltenes. The catalytic addition provided an increase in the content of light components, such as saturates and aromatics, of almost 10 wt%, while the share of heavy components, such as resins and asphaltenes, was reduced by 12.5 wt% The difference between the decrease in the content of the heavy fractions and the increase in the quantity of light fractions is explained by the formation of gaseous products. A small increase in the content of asphaltenes after catalytic upgrading probably refers to the lack of hydrogen that is capable of terminating the polymerization reactions.
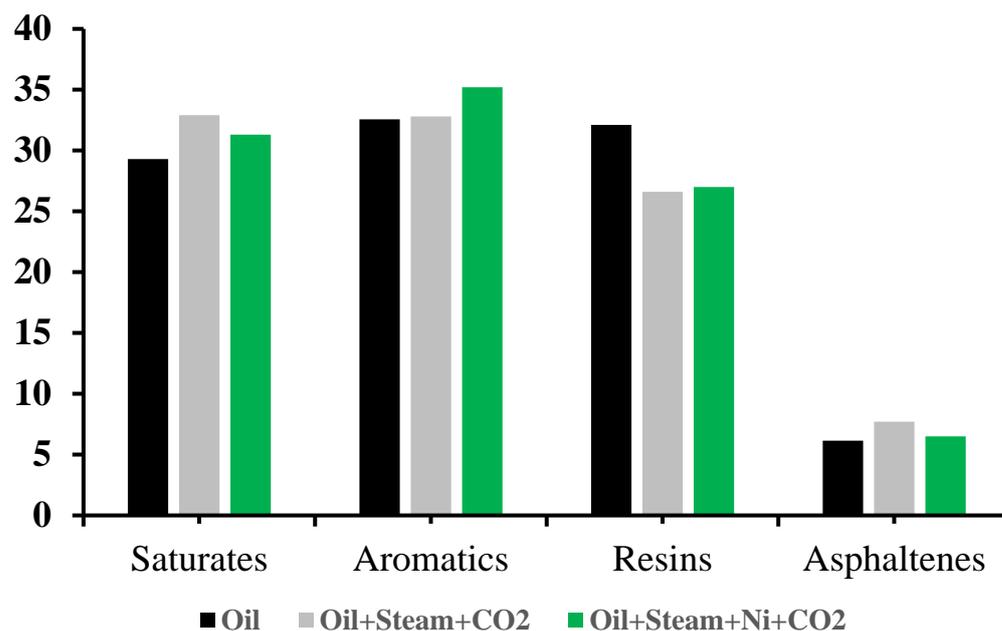

Figure 3. The chemical group composition of oil samples.

3.3. GC-MS Results of Saturates and Aromatics

The GC-MS results of the saturated fractions isolated from the initial crude oil sample, and after CO_2-assisted hydrothermal treatment at 300 °C, in both the absence and the presence of nickel tallate, are presented in Table 2 and Figure 4. The relative content of C10–C20 n-alkanes increased from 6.30% to 10.93% in the case of the noncatalytic upgrading. The addition of the catalyst further increased this value by up to 11.8%. This is explained by the destruction of the aliphatic C-C bonds in the long-chain normal alkanes. It also can be referred to the detachment of alkyl substitutes from the asphaltene fragments as a result of the radical chain mechanism or ring-opening reactions. Apparently, the nickel-based catalyst promoted these reactions.

Table 2. The relative content of n-alkanes in the composition of the saturates of the oil, before and after the noncatalytic and catalytic hydrothermal processes.

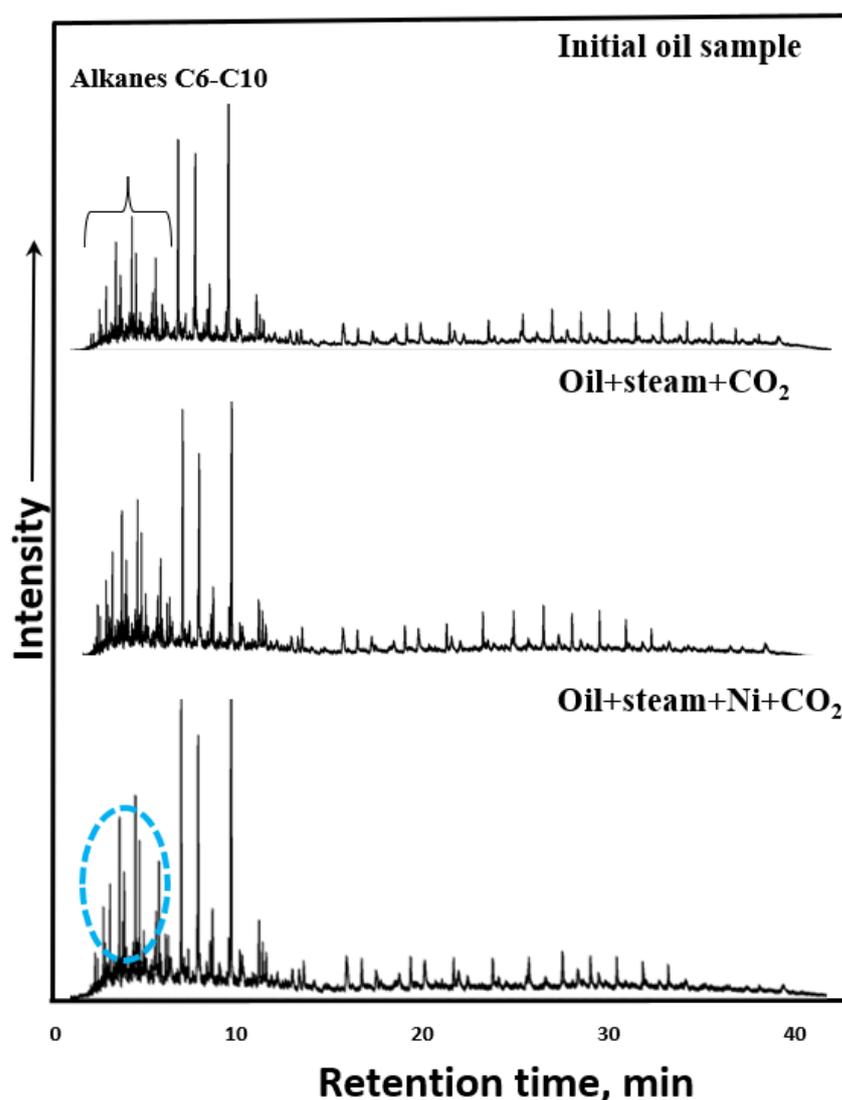| Samples	Oil	Oil + Steam + CO_2	Oil + Steam + Ni + CO_2
n-alkanes C10–C20	6.30	10.93	11.80
n-alkanes C21–C34	20.80	17.96	19.12
isoalkanes	72.90	71.11	69.08

Figure 4. The GC-MS spectra of saturates.

The GC-MS spectra of the fractions of the aromatics are illustrated in Figure 5. The noncatalytic hydrothermal treatment of crude oil in a CO_2 medium led to the absence of some peaks in the composition of the aromatics, which is probably due to the polymerization of some polyaromatic hydrocarbons. According to the results of the SARA analysis, the condensed aromatic rings probably transferred to the fraction of asphaltenes.

Figure 6 shows the 1,3,4-trimethyl-2-alkylbenzenes identified by $m/z = 133$ in order to clearly demonstrate the changes in the distribution of the heavy aromatic components. It was found that the intensity of the 1,3,4-trimethyl-2-alkylbenzenes with the alkyl substitution of C4 ($C_{13}H_{20}$) was lesser than that of the C5 ($C_{14}H_{22}$) in the composition of the initial oil sample. However, the catalytic destructive hydrogenation of asphaltenes led to

the increase in the content of 1,3,4-trimethyl-2-alkylbenzenes with the alkyl substitution of C4 ($C_{13}H_{20}$), in contrast to the CX=C5 ($C_{14}H_{22}$).

Naphthalene and its homologues were evaluated by m/z = 128, 142, 156, and 170. The obtained mass spectra are illustrated in Figure 7. The naphthalene and its homologues became poor because of the polymerization reactions, which were significant in the absence of the catalyst. The ratio between 2,3,6-trimethylnaphthalene and 1,6,7-trimethylnaphthalene changed after the catalytic steam treatment, which also indicates the destruction of asphaltene fragments.

Phenanthrenes, methyl phenanthrenes, and trimethyl phenanthrenes were isolated from the TIC by m/z = 178, 192, and 206. The achieved spectra are presented in Figure 8. The intensities of all of the peaks in the model system without the catalyst are the lowest. A peak corresponding to 1-methyl-7-isopropylphenanthrene can be observed in the aromatic fraction of the upgraded oil sample in the presence of the catalyst. This is also a product of the destruction of asphaltene fragments.
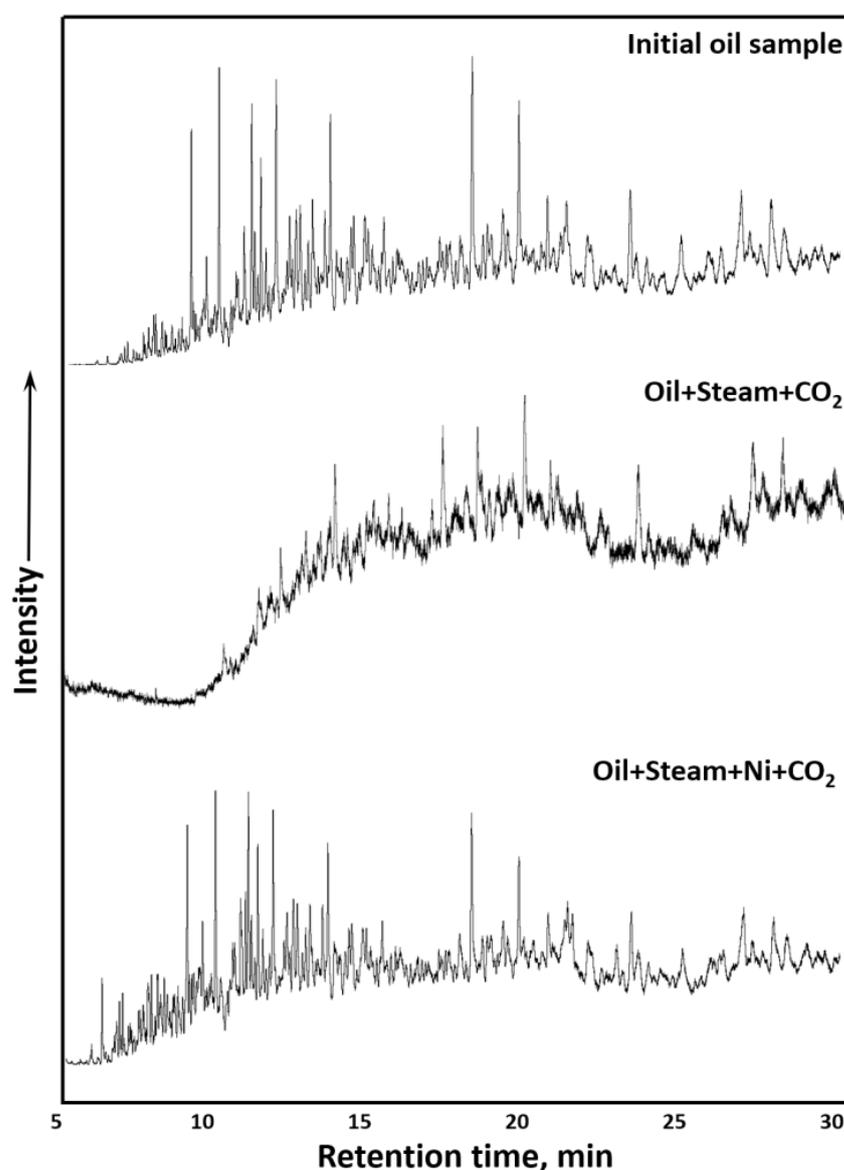

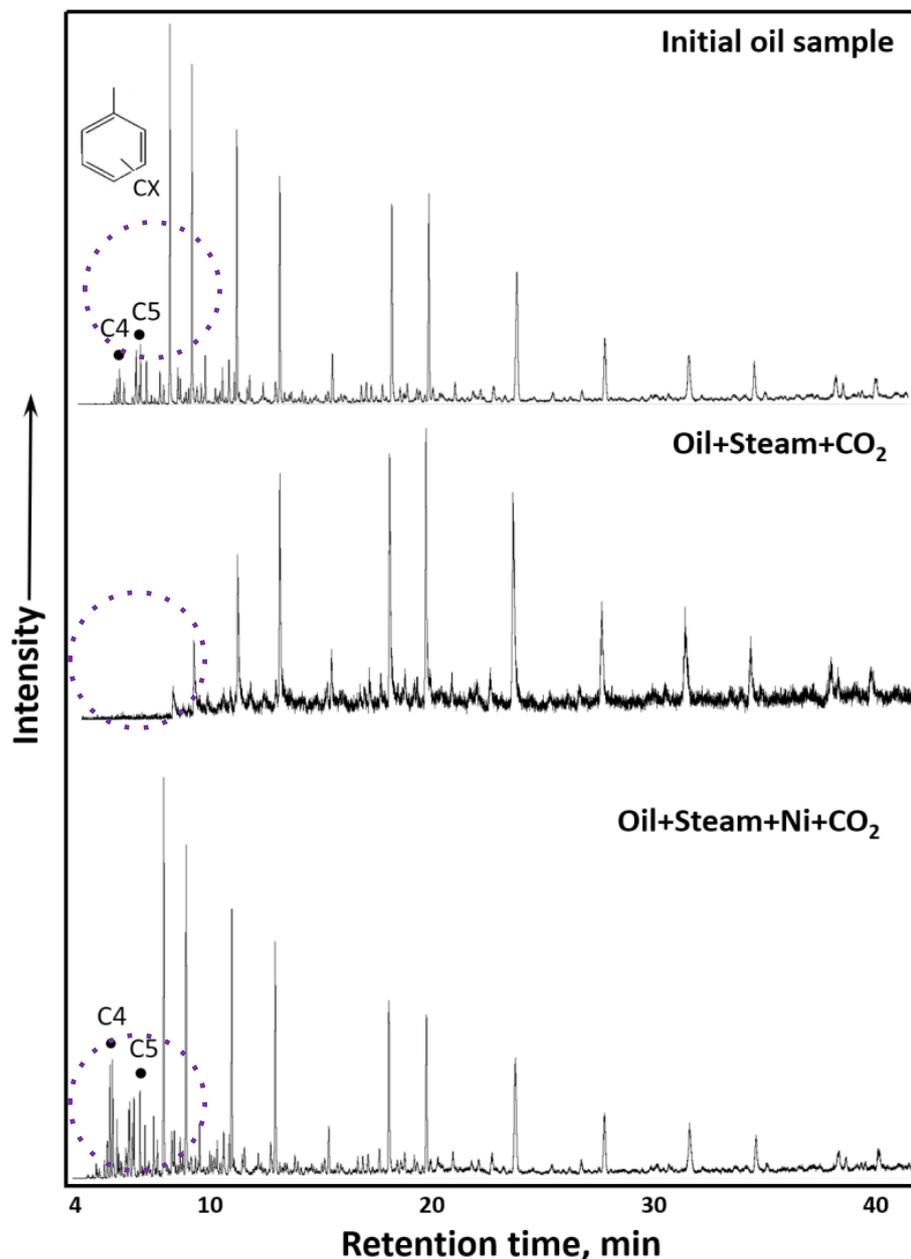**Figure 5.** GC-MS spectra of the fractions of aromatics.

Figure 6. GC-MS spectra of 1,3,4-trimethyl-2-alkylbenzenes.

3.4. Viscosity Measurements of Oil Samples

Rheology of the heavy crude oil samples in general showed non-Newtonian behavior as viscosity alteration was observed by increasing shear rate. However, after a certain speed, $0.8\,s^{-1}$, all samples exhibited the behavior of a Newtonian flow. The noncatalytic hydrogenation of CO_2 led to a reduction of the viscosity value from 3309 mPa·s to 1775 mPa·s at a shear rate of $0.66\,s^{-1}$. The catalytic hydrogenation of the CO_2 further reduced viscosity down to 1167 mPa·s at the given shear rate (Figure 9). The heavy oil viscosity-reduction mechanism has two paths: chemical and physical. The hydrogenation of carbon dioxide results in the formation of light hydrocarbons and methane. Moreover, the high molecular components of heavy oil, such as resins and asphaltenes, undergo destructive hydrogenation. All of these processes have a significant influence on viscosity reduction. On the other hand, chemically unreacted CO_2 can physically affect the viscosity of heavy oil by dissolving in it. The injected CO_2 under the steam conditions became supercritical, and it

was totally miscible with the heavy crude oil sample. Thus, the alteration of the wetting and interfacial properties can additionally contribute to heavy oil production.

3.5. FTIR Spectroscopy Results of Oil Samples

The FTIR spectra of the heavy oil samples, before and after catalytic and noncatalytic hydrogenation of CO_2, are presented in Figure 10. The spectral coefficients were calculated to compare the changes in the structure of the crude oil samples. They are defined as the ratio of absorption values at the maximum of the corresponding absorption bands: C1 = A1600/A720 (aromaticity), C2 = A1710/A1465 (oxidation), C3 = A1380/A1465 (branching), C4 = (A720 + A1380)/A1600 (saturated), and C5 = A1030/A1465 (sulfurization). The estimated results are summarized in Table 3.
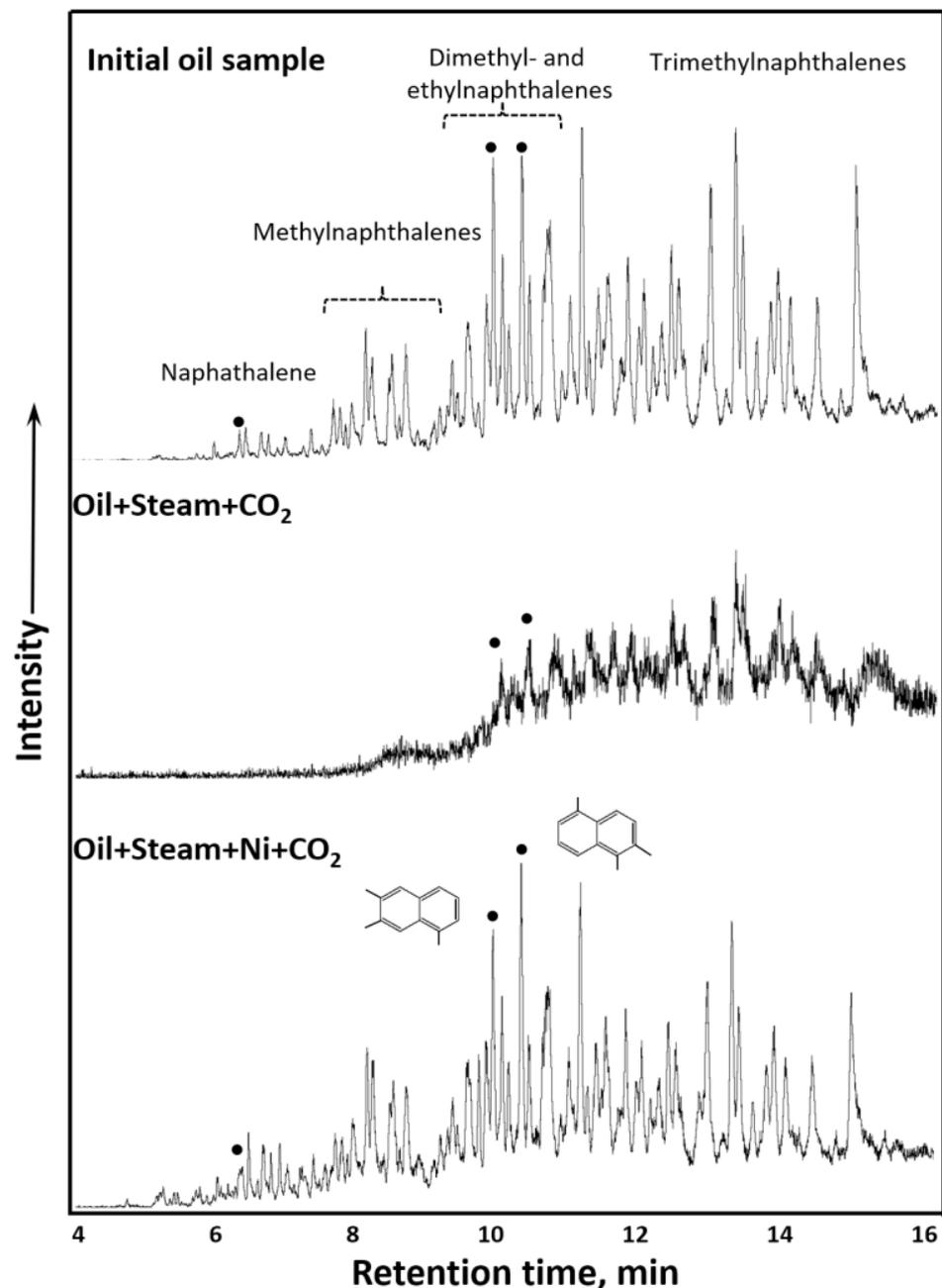

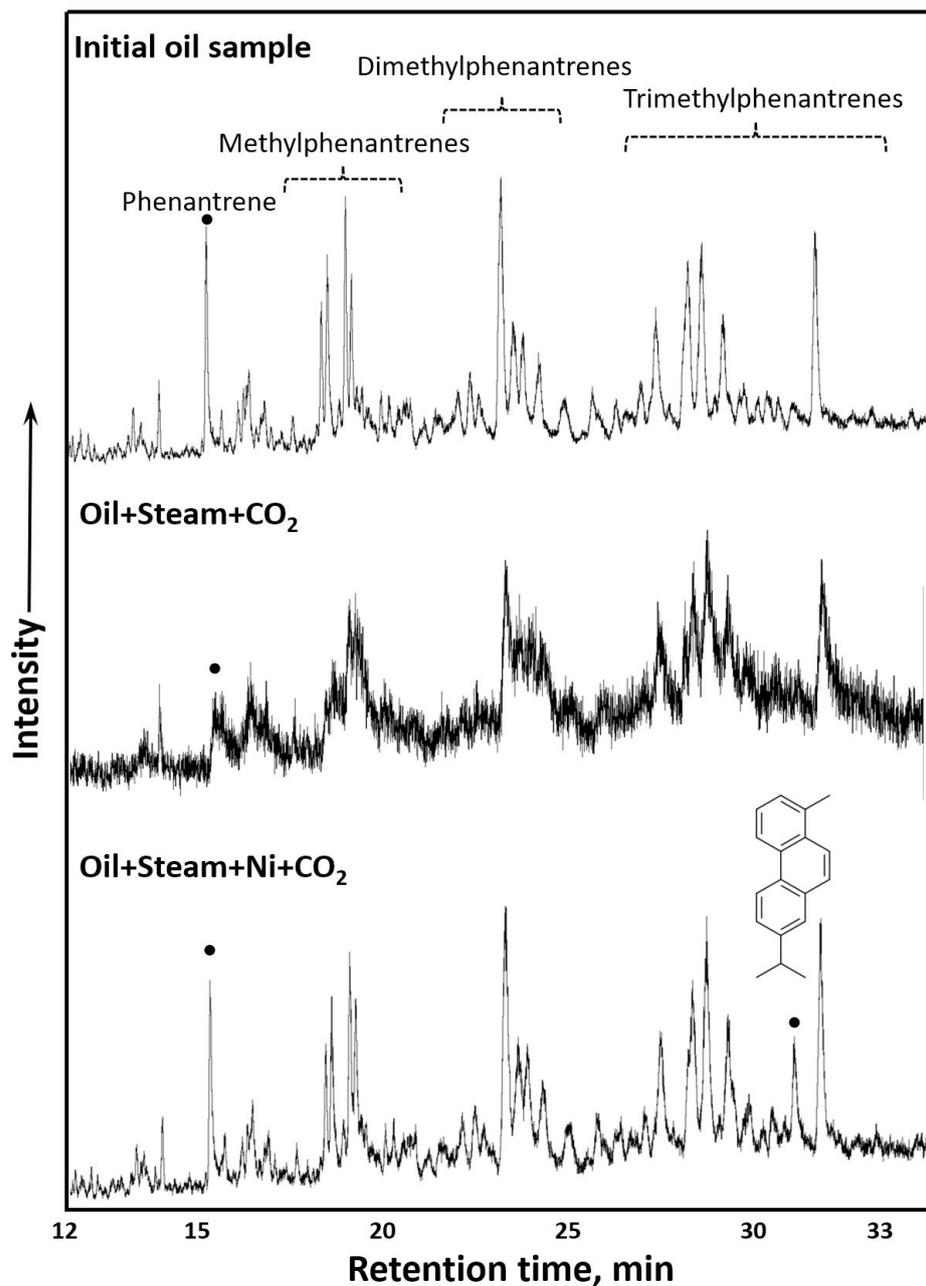**Figure 7.** GC-MS spectra of naphthalene.

Figure 8. GC-MS spectra of phenanthrenes.

Table 3. FTIR spectral coefficients of oil samples, before and after noncatalytic and catalytic hydrothermal processes.

* Spectral Coefficients	Subject of Research		
	Initial Crude Oil	Oil + Steam + CO_2	Oil + Steam + Ni + CO_2
C_1	0.43	0.43	0.44
C_2	0.03	0.05	0.12
C_3	0.62	0.62	0.63
C_4	6.80	6.54	5.31
C_5	0.17	0.20	0.18

* C_1 = D1600/D720 (aromaticity); C2 = D1710/D1465 (oxidation); C3 = D1380/D1465 (branching); C4 = (D720 + D1380)/D1600 (aliphaticity); C5 = D1030/D1465 (sulfurization index).

According to the spectra and calculated spectral coefficients, the addition of the catalyst provided an increase in aromaticity (C1) due to the destruction of peripheral aliphatic hydrocarbons (C4). The branching (C3) of the heavy crude oil samples, before and after hydrogenation of CO_2, is almost the same. The sulfurization index (C5) in the case of the nickel catalyst is lower than that of the control sample, which is explained by the transformation of nickel oxides to nickel sulfides.
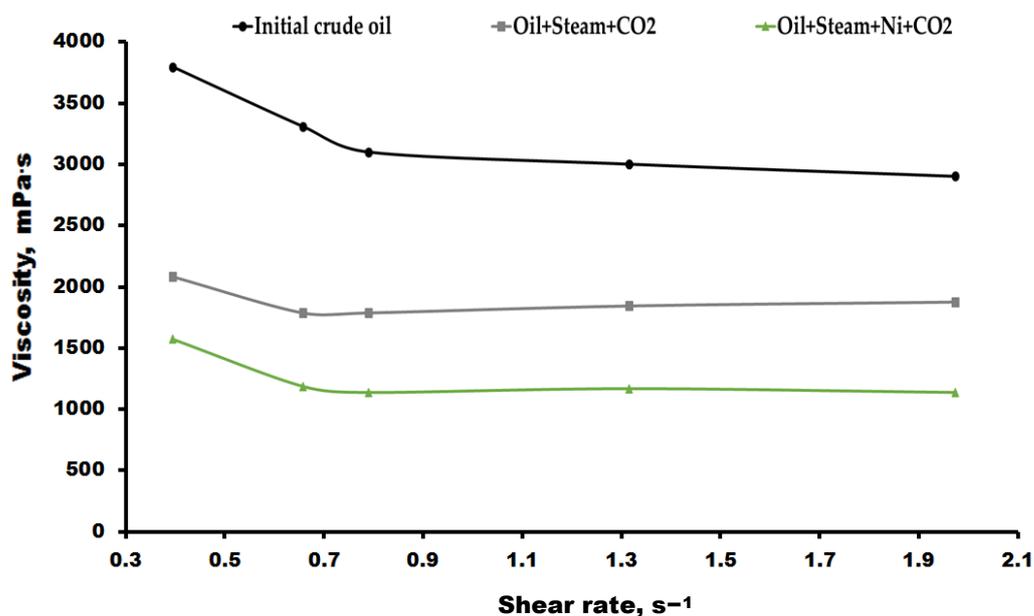

Figure 9. Shear rate-dependent viscosity values, before and after noncatalytic and catalytic CO_2-assisted hydrothermal upgrading.
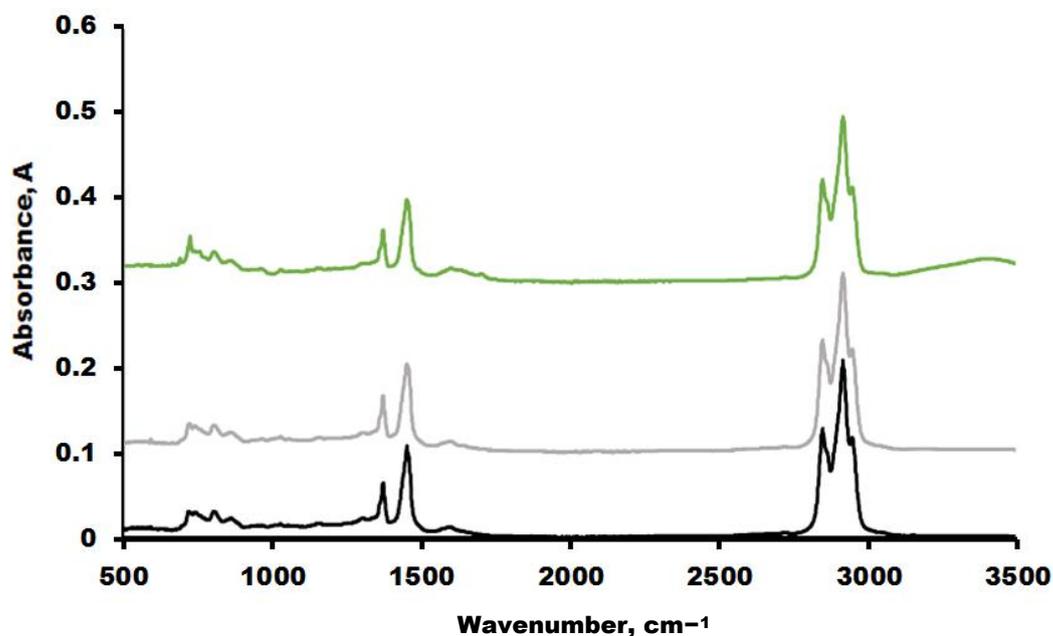

Figure 10. FTIR spectra of heavy oil samples, before and after catalytic and noncatalytic hydrogenation of CO_2.

4. Conclusions

In this study, laboratory stimulation experiments were implemented to imitate the in-situ utilization of carbon dioxide by hydrogenation processes. Moreover, the catalytic conversion products of carbon dioxide assisted in upgrading the heavy oil and thus en-

hanced heavy oil production. The experimental results showed the catalytic activity of nickel tallate on hydrogenation of carbon dioxide at 300 °C and 90 bar. According to the GC results, the amount of CO_2 involved in the hydrogenation processes was doubled in the presence of the catalyst. Moreover, the formation of methane was suppressed in the presence of the catalyst, while the contents of ethane and propane were increased in contrast with those of the blank sample. The group composition of the heavy crude oil sample was improved. The content of the light components was increased, and the share of the heavy components, such as resins and asphaltenes, was reduced by 12.5 wt% The relative content of normal C10–C20 alkanes in saturates was increased from 6.30% to 11.8% with the addition of the catalysts. The noncatalytic steam conversion of CO_2 led to the reduction of viscosity from 3309 mPa·s to 1775 mPa·s at a shear rate of 0.66 s^{-1}, while the catalytic hydrogenation of CO_2 further reduced the viscosity to 1167 mPa·s at the same shear rate. Thus, the in situ hydrogenation of CO_2 is an effective method for the utilization of carbon dioxide and the enhancement of thermal heavy oil production.

Author Contributions: Conceptualization, F.A. and A.V.; methodology, O.S.; investigation, T.K. and O.M.; writing—F.A.; review and editing, F.A. and T.K. All authors have read and agreed to the published version of the manuscript.

Institutional Review Board Statement: Not applicable.

Informed Consent Statement: Not applicable.

Data Availability Statement: Not applicable.

Conflicts of Interest: The authors declare no conflict of interest.

References

1. Rogelj, J.; den Elzen, M.; Höhne, N.; Fransen, T.; Fekete, H.; Winkler, H.; Schaeffer, R.; Sha, F.; Riahi, K.; Meinshausen, M. Paris Agreement Climate Proposals Need a Boost to Keep Warming Well below 2 C. *Nature* **2016**, *534*, 631–639. [CrossRef] [PubMed]
2. Tarkowski, R.; Uliasz-Misiak, B.; Tarkowski, P. Storage of Hydrogen, Natural Gas, and Carbon Dioxide–Geological and Legal Conditions. *Int. J. Hydrogen Energy* **2021**, *46*, 20010–20022. [CrossRef]
3. Raza, A.; Gholami, R.; Rezaee, R.; Rasouli, V.; Rabiei, M. Significant Aspects of Carbon Capture and Storage—A Review. *Petroleum* **2019**, *5*, 335–340. [CrossRef]
4. Aminu, M.D.; Nabavi, S.A.; Rochelle, C.A.; Manovic, V. A Review of Developments in Carbon Dioxide Storage. *Appl. Energy* **2017**, *208*, 1389–1419. [CrossRef]
5. Alcorn, Z.P.; Fredriksen, S.B.; Sharma, M.; Rognmo, A.U.; Føyen, T.L.; Fernø, M.A.; Graue, A. An Integrated Carbon-Dioxide-Foam Enhanced-Oil-Recovery Pilot Program with Combined Carbon Capture, Utilization, and Storage in an Onshore Texas Heterogeneous Carbonate Field. *SPE Reserv. Eval. Eng.* **2019**, *22*, 1449–1466. [CrossRef]
6. Bondor, P.L. Applications of Carbon Dioxide in Enhanced Oil Recovery. *Energy Convers. Manag.* **1992**, *33*, 579–586. [CrossRef]
7. Blunt, M.; Fayers, F.J.; Orr, F.M., Jr. Carbon Dioxide in Enhanced Oil Recovery. *Energy Convers. Manag.* **1993**, *34*, 1197–1204. [CrossRef]
8. Wei, J.; Zhou, J.; Li, J.; Zhou, X.; Dong, W.; Cheng, Z. Experimental Study on Oil Recovery Mechanism of CO_2 Associated Enhancing Oil Recovery Methods in Low Permeability Reservoirs. *J. Pet. Sci. Eng.* **2021**, *197*, 108047. [CrossRef]
9. Gunasekar, G.H.; Park, K.; Jung, K.-D.; Yoon, S. Recent Developments in the Catalytic Hydrogenation of CO_2 to Formic Acid/Formate Using Heterogeneous Catalysts. *Inorg. Chem. Front* **2016**, *3*, 882–895. [CrossRef]
10. Zhou, G.; Dai, B.; Xie, H.; Zhang, G.; Xiong, K.; Zheng, X. CeCu Composite Catalyst for CO Synthesis by Reverse Water–Gas Shift Reaction: Effect of Ce/Cu Mole Ratio. *J. CO$_2$ Util.* **2017**, *21*, 292–301. [CrossRef]
11. Lee, M.-D.; Lee, J.-F.; Chang, C.-S. Hydrogenation of Carbon Dioxide on Unpromoted and Potassium-Promoted Iron Catalysts. *Bull. Chem. Soc. Jpn.* **1989**, *62*, 2756–2758. [CrossRef]
12. Prieto, G. Carbon Dioxide Hydrogenation into Higher Hydrocarbons and Oxygenates: Thermodynamic and Kinetic Bounds and Progress with Heterogeneous and Homogeneous Catalysis. *ChemSusChem* **2017**, *10*, 1056–1070. [CrossRef] [PubMed]
13. Nakayama, T.; Ichikuni, N.; Sato, S.; Nozaki, F. Ni/MgO Catalyst Prepared Using Citric Acid for Hydrogenation of Carbon Dioxide. *Appl. Catal. A Gen.* **1997**, *158*, 185–199. [CrossRef]
14. Ayodele, O.B. Eliminating Reverse Water Gas Shift Reaction in CO_2 Hydrogenation to Primary Oxygenates over MFI-Type Zeolite Supported Cu/ZnO Nanocatalysts. *J. CO$_2$ Util.* **2017**, *20*, 368–377. [CrossRef]

15. Su, X.; Yang, X.; Zhao, B.; Huang, Y. Designing of Highly Selective and High-Temperature Endurable RWGS Heterogeneous Catalysts: Recent Advances and the Future Directions. *J. Energy Chem.* **2017**, *26*, 854–867. [CrossRef]

16. Ma, J.; Sun, N.; Zhang, X.; Zhao, N.; Xiao, F.; Wei, W.; Sun, Y. A Short Review of Catalysis for CO_2 Conversion. *Catal. Today* **2009**, *148*, 221–231. [CrossRef]

17. Guo, R.; Fu, W.; Qu, L.; Li, Y.; Yuan, W.; Chen, G. Methanol-Enhanced Fe (III) Oleate-Catalyzed Aquathermolysis of Heavy Oil. *Processes* **2022**, *10*, 1956. [CrossRef]

18. Kattel, S.; Liu, P.; Chen, J.G. Tuning Selectivity of CO_2 Hydrogenation Reactions at the Metal/Oxide Interface. *J. Am. Chem. Soc.* **2017**, *139*, 9739–9754. [CrossRef]

19. Ma, L.; Zhang, S.; Zhang, X.; Dong, S.; Yu, T.; Slaný, M.; Chen, G. Enhanced Aquathermolysis of Heavy Oil Catalysed by Bentonite Supported Fe (III) Complex in the Present of Ethanol. *J. Chem. Technol. Biotechnol.* **2022**, *97*, 1128–1137. [CrossRef]

20. Beuls, A.; Swalus, C.; Jacquemin, M.; Heyen, G.; Karelovic, A.; Ruiz, P. Methanation of CO_2: Further Insight into the Mechanism over Rh/γ-Al_2O_3 Catalyst. *Appl. Catal. B* **2012**, *113*, 2–10. [CrossRef]

21. da Silva, D.C.D.; Letichevsky, S.; Borges, L.E.P.; Appel, L.G. The Ni/ZrO_2 Catalyst and the Methanation of CO and CO_2. *Int. J. Hydrogen Energy* **2012**, *37*, 8923–8928. [CrossRef]

22. Razzaq, R.; Li, C.; Usman, M.; Suzuki, K.; Zhang, S. A Highly Active and Stable Co4N/γ-Al_2O_3 Catalyst for CO and CO_2 Methanation to Produce Synthetic Natural Gas (SNG). *Chem. Eng. J.* **2015**, *262*, 1090–1098. [CrossRef]

23. Pastor-Pérez, L.; Baibars, F.; le Sache, E.; Arellano-Garcia, H.; Gu, S.; Reina, T.R. CO_2 Valorisation via Reverse Water-Gas Shift Reaction Using Advanced Cs Doped Fe-Cu/Al_2O_3 Catalysts. *J. CO_2 Util.* **2017**, *21*, 423–428. [CrossRef]

24. Zhu, M.; Wachs, I.E. Resolving the Reaction Mechanism for H_2 Formation from High-Temperature Water–Gas Shift by Chromium–Iron Oxide Catalysts. *ACS Catal.* **2016**, *6*, 2827–2830. [CrossRef]

25. Loiland, J.A.; Wulfers, M.J.; Marinkovic, N.S.; Lobo, R.F. Fe/γ-Al_2O_3 and Fe–K/γ-Al_2O_3 as Reverse Water-Gas Shift Catalysts. *Catal. Sci. Technol.* **2016**, *6*, 5267–5279. [CrossRef]

26. Park, S.-W.; Joo, O.-S.; Jung, K.-D.; Kim, H.; Han, S.-H. ZnO/Cr_2O_3 Catalyst for Reverse-Water-Gas-Shift Reaction of CAMERE Process. *Korean J. Chem. Eng.* **2000**, *17*, 719–722. [CrossRef]

27. Feng, K.; Tian, J.; Guo, M.; Wang, Y.; Wang, S.; Wu, Z.; Zhang, J.; He, L.; Yan, B. Experimentally Unveiling the Origin of Tunable Selectivity for CO_2 Hydrogenation over Ni-Based Catalysts. *Appl. Catal. B* **2021**, *292*, 120191. [CrossRef]

28. Sengupta, S.; Jha, A.; Shende, P.; Maskara, R.; Das, A.K. Catalytic Performance of Co and Ni Doped Fe-Based Catalysts for the Hydrogenation of CO_2 to CO via Reverse Water-Gas Shift Reaction. *J. Environ. Chem. Eng.* **2019**, *7*, 102911. [CrossRef]

29. Wang, C.; Tian, Y.; Wu, R.; Li, H.; Yao, B.; Zhao, Y.; Xiao, T. Bimetallic Synergy Effects of Phyllosilicate-Derived NiCu@ SiO_2 Catalysts for 1,4-Butynediol Direct Hydrogenation to 1,4-Butanediol. *ChemCatChem* **2019**, *11*, 4777–4787. [CrossRef]

30. Vakhin, A.V.; Aliev, F.A.; Mukhamatdinov, I.I.; Sitnov, S.A.; Sharifullin, A.V.; Kudryashov, S.I.; Afanasiev, I.S.; Petrashov, O.V.; Nurgaliev, D.K. Catalytic Aquathermolysis of Boca de Jaruco Heavy Oil with Nickel-Based Oil-Soluble Catalyst. *Processes* **2020**, *8*, 532. [CrossRef]

31. Al-Muntaser, A.A.; Varfolomeev, M.A.; Suwaid, M.A.; Feoktistov, D.A.; Yuan, C.; Klimovitskii, A.E.; Gareev, B.I.; Djimasbe, R.; Nurgaliev, D.K.; Kudryashov, S.I. Hydrogen Donating Capacity of Water in Catalytic and Non-Catalytic Aquathermolysis of Extra-Heavy Oil: Deuterium Tracing Study. *Fuel* **2021**, *283*, 118957. [CrossRef]

32. Sitnov, S.A.; Mukhamatdinov, I.I.; Vakhin, A.V.; Ivanova, A.G.; Voronina, E.V. Composition of Aquathermolysis Catalysts Forming in Situ from Oil-Soluble Catalyst Precursor Mixtures. *J. Pet. Sci. Eng.* **2018**, *169*, 44–50. [CrossRef]